ChemPubSoc Europe

DOI: 10.1002/cphc.201201069

Electron Transfer between Hydrogen-Bonded Pyridylphenols and a Photoexcited Rhenium(I) Complex

William Herzog,[b] Catherine Bronner,[a] Susanne Löffler,[c] Bice He,[c] Daniel Kratzert,[c] Dietmar Stalke,[c] Andreas Hauser,[b] and Oliver S. Wenger*[a]

Two pyridylphenols with intramolecular hydrogen bonds between the phenol and pyridine units have been synthesized, characterized crystallographically, and investigated by cyclic voltammetry and UV/Vis spectroscopy. Reductive quenching of the triplet metal-to-ligand charge-transfer excited state of the $[Re(CO)_3(phen)(py)]^+$ complex (phen = 1,10-phenanthroline, py = pyridine) by the two pyridylphenols and two reference phenol molecules is investigated by steady-state and time-resolved luminescence spectroscopy, as well as by transient absorption spectroscopy. Stern–Volmer analysis of the luminescence quenching data provides rate constants for the bimolecular excited-state quenching reactions. H/D kinetic isotope effects for the pyridylphenols are on the order of 2.0, and the bimolecular quenching reactions are up to 100 times faster with the pyridylphenols than with the reference phenols. This observation is attributed to the markedly less positive oxidation potentials of the pyridylphenols with respect to the reference phenols (≈0.5 V), which in turn is caused by proton coupling of the phenol oxidation process. Transient absorption spectroscopy provides unambiguous evidence for the photogeneration of phenoxyl radicals, that is, the overall photoreaction is clearly a proton-coupled electron-transfer process.

1. Introduction

The tyrosine Z (Tyr_Z)/histidine 190 (His190) pair of photosystem II is one of the best-known hydrogen-bonded phenol systems in chemistry.[1] Numerous experimental and theoretical investigations have been geared at understanding the proton-coupled electron transfer (PCET) chemistry of the Tyr_Z/His190 reaction couple, many of them focusing on simple artificial model compounds in which a phenol unit can form intramolecular hydrogen bonds to a nitrogen base.[2] A wide range of experimental methods have been applied, including EPR,[3] electrochemical,[4] and optical spectroscopic studies.[5] However, in most cases the phenol oxidation process involves oxidants that are in their electronic ground states, and there are comparatively few studies in which the oxidant is an electronically excited molecule.[5b,6]

Against this background we deemed it interesting to explore the photoredox chemistry between hydrogen-bonded phenol molecules and a photoexcited rhenium(I) tricarbonyl diimine complex, which is known to be a potent excited-state oxidant.[6e,7] The molecular structures of our model systems are shown in Scheme 1. The rhenium(I) complex has a 1,10-phenanthroline (phen) and a pyridine (py) ligand in addition to the three carbonyl groups; the phenol reaction partners have pendant pyridine units that are connected through a $-CH_2-$ group to disrupt π conjugation between the two aromatic subunits. One of the phenol groups contains no further substituents ($PhOH-CH_2$-py) whereas the other has *tert*-butyl groups at the 4- and 6-positions ($tBu_2PhOH-CH_2$-py). We anticipated that if excited to its long-lived triplet metal-to-ligand charge-transfer (^{3}MLCT) state the rhenium(I) complex would be capable of inducing intermolecular electron transfer (ET) with the phenol, and this process should be accompanied by intramolecular proton transfer (PT) between the phenol and the pyridine.

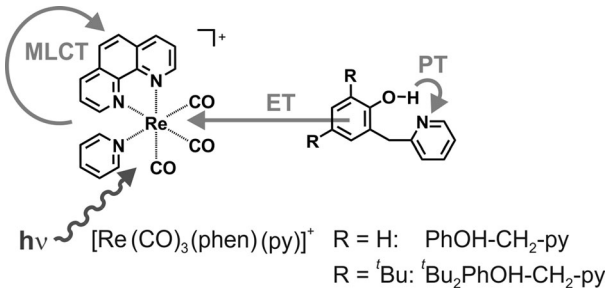

Scheme 1. Molecular structures of the photosensitizer/quencher pairs with the two hydrogen-bonded phenol molecules of central interest to this study. hν = light excitation; MLCT = metal-to-ligand charge transfer; ET = electron transfer; PT = proton transfer.

[a] Dr. C. Bronner, Prof. O. S. Wenger
Departement für Chemie
Universität Basel
Spitalstrasse 51, 4056 Basel (Switzerland)
E-mail: oliver.wenger@unibas.ch

[b] Dr. W. Herzog, Prof. A. Hauser
Département de Chimie Physique
Université de Genève
30 quai Ernest-Ansermet, 1211 Genève 4 (Switzerland)

[c] S. Löffler, Dr. B. He, D. Kratzert, Prof. D. Stalke
Institut für Anorganische Chemie
Georg-August Universität
Tammannstrasse 4, 37077 Göttingen (Germany)

Supporting information for this article is available on the WWW under http://dx.doi.org/10.1002/cphc.201201069.

The PCET chemistry of tBu$_2$PhOH-CH$_2$-py with various oxidants in their electronic ground states has been found previously to occur through a concerted proton–electron transfer (CPET) mechanism.[2e,5c–f] Herein, we focus specifically on the excited-state PCET chemistry between $[Re(CO)_3(phen)(py)]^+$ and PhOH-CH$_2$-py or tBu$_2$PhOH-CH$_2$-py. As reference phenols without the possibility of forming intramolecular hydrogen bonds we used ordinary phenol (PhOH) and 2,4-di-*tert*-butylphenol (tBu$_2$PhOH).

2. Results and Discussion

Synthesis

The synthesis of tBu$_2$PhOH-CH$_2$-py had been previously described,[5c,d,f] but in our hands a different procedure turned out to be more convenient for obtaining the two pyridylphenols from Scheme 1.[8] Our synthetic strategy is illustrated in Scheme 2 and begins with commercially available 2-bromophenols (**1** and **3**), which are methylated to protect the phenolic function for the subsequent reaction step. The protected phenols (**2** and **4**) are reacted with pyridine molecule **5** (which is accessible in one step from 2-picoline and diisopropyl ketone) by using a palladium catalyst.[8] The coupling products (**6** and **8**) are deprotected with aqueous HBr (in the case of **6**)[9] or ethanethiol (in the case of **8**)[10] to obtain the final pyridylphenols (**7**, PhOH-CH$_2$-py and **9**, tBu$_2$PhOH-CH$_2$-py).

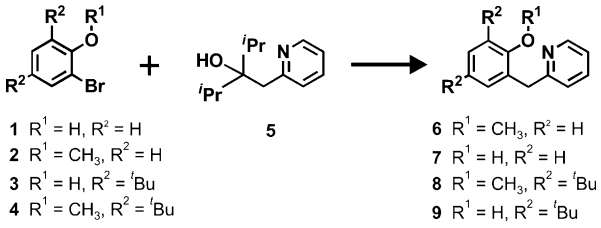

Scheme 2. Synthesis of the two pyridylphenols from Scheme 1.

Crystal Structures

Figure 1 (top) shows the crystal structure of PhOH-CH$_2$-py, which crystallizes in the monoclinic space group $C2/c$ with one molecule in the asymmetric unit. The molecules in the crystal lattice of PhOH-CH$_2$-py are connected through intermolecular hydrogen bonds between the phenolic OH group and the nitrogen of the pyridyl ring. These bonds generate a zigzag-like chain along the b axis of the crystal lattice. The position of the hydrogen atom was modeled as a riding atom with a fixed distance of 0.84 Å and a freely refined torsion angle. The resulting hydrogen bond is slightly bent with 175° for the O–H–N angle and has a H–N distance of 1.90 Å, which results in a total O–H–N distance of 2.740(2) Å. Figure 1 (bottom) shows the crystal structure of tBu$_2$PhOH-CH$_2$-py, which crystallizes in the monoclinic space group $P2_1/n$ with one molecule in the asymmetric unit. One of the tBu groups happens to be disordered by 5%. This molecule only forms an intramolecular hydrogen bond between H1 and N1. The hydrogen H1 was found in the difference Fourier density. The position and isotropic vibration were refined freely with a distance restraint of 0.84(2) Å to O1. The O–H distance refined to 0.88(2) Å with a N–H distance of 1.827(16) Å and a total O–N distance of 2.6956(16) Å with an O–H–N angle of 169(2)°. Thus, there is clear evidence for hydrogen-bonding interactions in the crystal structures of PhOH-CH$_2$-py and tBu$_2$PhOH-CH$_2$-py.[11] A structure of tBu$_2$PhOH-CH$_2$-py had been published previously.[5f]

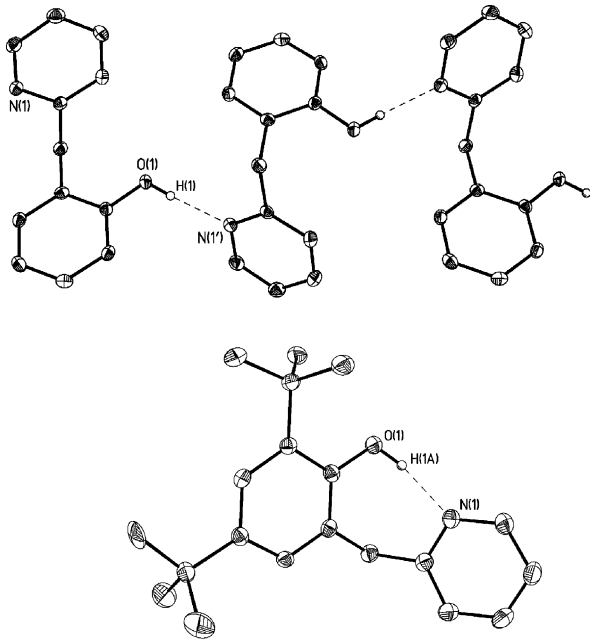

Figure 1. Crystal structures of PhOH-CH$_2$-py (top) and tBu$_2$PhOH-CH$_2$-py (bottom). Anisotropic displacement parameters are depicted at the 50% probability level. Selected bond lengths and angles can be found in the Supporting Information.

Intramolecular Hydrogen Bonding in Solution

^{1}H NMR spectra of the two pyridylphenols in $CDCl_3$ exhibit sharp downfield resonances for the phenolic protons, specifically at $\delta = 11.67$ ppm for PhOH-CH$_2$-py and at $\delta = 11.40$ ppm for tBu$_2$PhOH-CH$_2$-py, which is typical for intramolecularly hydrogen-bonded phenols.[12] We conclude that intramolecular hydrogen bonds are not only present in one of our solid-state structures but also in aprotic solution.

Cyclic Voltammetry

Figure 2 shows cyclic voltammograms of tBu$_2$PhOH, tBu$_2$PhOH-CH$_2$-py, and PhOH-CH$_2$-py in dry CH_2Cl_2 in the presence of 0.1 M tetrabutylammonium hexafluorophosphate ($TBAPF_6$) electrolyte. The reversible waves at 0.0 V versus ferrocenium/ferrocene (Fc^+/Fc; dashed vertical line in Figure 2) are due to ferrocene, which was added in small quantities for internal voltage calibration. The voltammogram of the reference phenol (Figure 2a) exhibits an irreversible oxidation wave peaking at 1.05 V versus Fc^+/Fc, which is typical for ordinary phenols be-

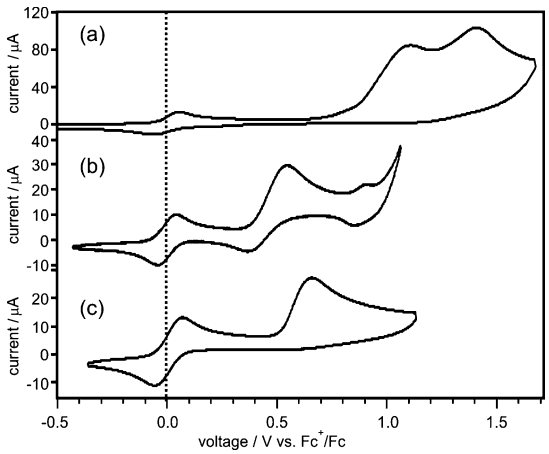

Figure 2. Cyclic voltammograms of the hydrogen-bonded phenols from Scheme 1 in dry CH_2Cl_2 in the presence of 0.1 M $TBAPF_6$. a) tBu$_2$PhOH; b) tBu$_2$PhOH-CH_2-py; c) PhOH-CH_2-py. The reversible waves at 0.0 V versus Fc^+/Fc are due to ferrocene, which was added in small quantities for internal voltage calibration; the scan rate was 100 mV s^{-1}.

cause the OH proton is lost to the bulk solution in the course of oxidation.[13]

The tBu$_2$PhOH-CH_2-py molecule, by contrast, exhibits a voltammogram in which the oxidative peak current near 0.5 V versus Fc^+/Fc is roughly 6 times larger than the corresponding reductive peak current. Their voltage separation is 170 mV but depends on the voltage sweep rate. The voltammogram in Figure 2b is qualitatively similar to that previously reported for the same compound in CH_3CN solution.[5c] The shape of this voltammogram can be explained by the possibility of transferring the phenolic proton to the pendant pyridine base in the course of oxidation and back-transfer to the phenol unit during the subsequent reductive potential sweep. The middle between the oxidative and reductive peak currents in Figure 2b is taken as the oxidation potential of tBu$_2$PhOH-CH_2-py (Table 1). Importantly, the oxidation potential of tBu$_2$PhOH-CH_2-py in CH_2Cl_2 is about 0.5 V less positive than the oxidation potential of tBu$_2$PhOH, a fact that has been previously noted for CH_3CN solution.[5c,d] It has been demonstrated that the unusually low oxidation potential of tBu$_2$PhOH-CH_2-py and related hydrogen-bonded phenols is a direct manifestation of intramolecular PT accompanying electrochemical phenol oxidation; hydrogen bonding alone cannot account for the large magnitude of the oxidation potential shift.[5c,14]

Table 1. Electrochemical potentials (E) for oxidation of the four phenol molecules and for reduction of the photoexcited $[Re(CO)_3(phen)(py)]^+$ complex.

Redox couple	E [V vs Fc^+/Fc]
$PhOH^+$/PhOH	1.25[a][d]
PhOH-CH_2-py$^+$/PhOH-CH_2-py	0.66[b]
tBu$_2$PhOH$^+$/tBu$_2$PhOH	1.05[b]
tBu$_2$PhOH-CH_2-py$^+$/tBu$_2$PhOH-CH_2-py	0.54[b]
*$[Re(CO)_3(phen)(py)]^+$/$[Re(phen)(CO)_3(py)]$	0.77[c][d]

[a] From ref. [15], converted from volts versus saturated calomel electrode (SCE) to volts versus Fc^+/Fc by subtracting 0.38 V as described in ref. [16]. [b] Measured in this work, peak potentials from Figure 2, 0.1 M $TBAPF_6$ electrolyte in CH_2Cl_2. [c] From reference [6f]. [d] In CH_3CN. The previously reported value for tBu$_2$PhOH-CH_2-py is 0.44 V versus Fc^+/Fc in CH_3CN.[5f] The potential of tBu$_2$PhOH is in line with the value reported in ref. [17] (0.519 V vs normal hydrogen electrode; addition of 0.624 V (according to ref. [16]) gives 1.14 V vs Fc^+/Fc).

The cyclic voltammogram of PhOH-CH_2-py in Figure 2c exhibits an irreversible oxidation wave peaking at 0.66 V versus Fc^+/Fc (Table 1). Despite the presence of an intramolecular hydrogen bond, phenol oxidation is clearly irreversible in this case, possibly because of the absence of substituents at the 4- and 6-positions of the phenol. Chemical substituents in the *ortho* and *para* positions to the phenolic function are known to enhance the stability of phenoxyl radicals.[18] By analogy to the other pyridylphenol from Scheme 1, PhOH-CH_2-py is oxidized at a much less positive potential than the PhOH reference molecule; in this specific case the potential difference amounts to approximately 0.6 V (Table 1).

The electrochemistry of the $[Re(CO)_3(phen)(py)]^+$ complex and related rhenium(I) tricarbonyl diimines was explored extensively in the past.[7,19] In Table 1 we merely give the electrochemical potential for one-electron reduction of ^{3}MLCT-excited $[Re(CO)_3(phen)(py)]^+$ as reported in the literature.[6f]

Optical Absorption

Figure 3 shows UV/Vis spectra of the four phenols and the rhenium(I) complex from Scheme 1 in CH_2Cl_2 at 25 °C. The important message from Figure 3 is that all four phenols are spectroscopically innocent at wavelengths longer than 330 nm. Between 270 and 280 nm they exhibit absorptions as previously reported for other phenols; in the presence of covalently attached pyridine units the extinction between 270 and 280 nm increases because pyridine itself has weakly absorbing n–π* transitions occurring in this spectral range.[20] As reported previously, the $[Re(CO)_3(phen)(py)]^+$ complex exhibits a MLCT band with maxima at 380 and 336 nm, whereas the absorption maximum at 276 nm has been attributed to phenanthroline-based electronic transitions.[19a,b] The most important observation from Figure 3 is that with light of wavelength 410 nm we can selectively excite the $[Re(CO)_3(phen)(py)]^+$ complex even in the presence of a large excess of any of the four phenols.

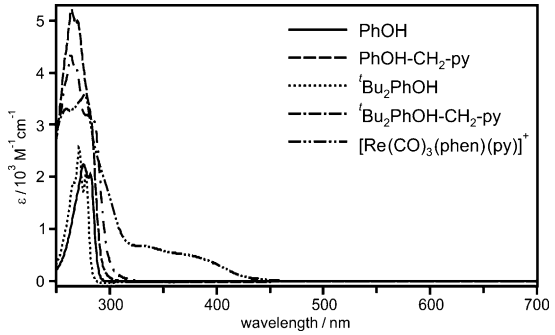

Figure 3. Optical absorption spectra of the four phenols and the rhenium(I) complex from Scheme 1.

Furthermore, there is no phenol absorption in the spectral range in which the rhenium(I) complex emits (450–700 nm); this is why in Figure 3 we show the entire spectral range between 250 and 700 nm. Note that phenol has a triplet energy (E_T) of 3.55 eV,[21] whereas the $[Re(CO)_3(phen)(py)]^+$ complex has $E_T \approx 2.75$ eV;[7,19a] hence, we can a priori rule out the possibility of ^{3}MLCT excited-state quenching by triplet–triplet energy transfer from $[Re(CO)_3(phen)(py)]^+$ to the phenols.[22]

Luminescence Quenching Experiments

The solid trace in Figure 4a is the emission spectrum of $[Re(CO)_3(phen)(py)]^+$ in aerated CH_2Cl_2 with 100 mM CH_3OH at 25 °C. The excitation wavelength was set at 410 nm. The broad and unstructured luminescence band is due to the typical

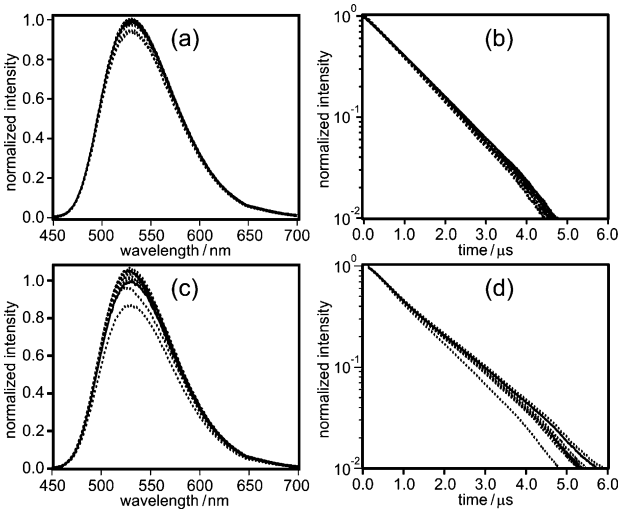

Figure 4. a) Luminescence of $[Re(CO)_3(phen)(py)]^+$ in aerated CH_2Cl_2 with 100 mM CH_3OH in the absence (——) and presence of increasing amounts of PhOH (•••••; 1–10 mM) after excitation at 410 nm. b) Luminescence decays of $[Re(CO)_3(phen)(py)]^+$ in the same solvent in the absence (——) and presence of increasing amounts of PhOH (•••••) after excitation at 410 nm with laser pulses of width approximately 10 ns (detection wavelength: 530 nm). c) The same experiment as in (a) but with deuterated phenol (PhOD) and 100 mM CH_3OD. d) The same experiment as in (b) but with deuterated phenol (PhOD) and 100 mM CH_3OD. All *y* axes are in arbitrary units; the intensity of the unquenched emission in (a) and (c) is normalized arbitrarily to 1; the intensity at $t = 0$ in (b) and (d) is normalized arbitrarily to 1.

^{3}MLCT emission of rhenium(I) tricarbonyl diimines.[19a] The solid trace in Figure 4b shows the temporal evolution of the ^{3}MLCT luminescence from Figure 4a after excitation with laser pulses of approximately 10 ns width at 410 nm; detection occurred at 530 nm. The luminescence intensity decays in a single-exponential manner over more than two orders of magnitude and a ^{3}MLCT lifetime of 1.2 μs is extracted, in line with previous reports.[19a,b] The dashed lines in Figure 4a,b were recorded in the presence of variable concentrations (1–10 mM) of PhOH. No significant luminescence quenching is observed with PhOH, neither in intensity (Figure 4a) nor in decay time (Figure 4b). Likewise, on using deuterated phenol (PhOD), the emission intensity stays virtually unchanged (Figure 4c) and the luminescence decays are no faster than in the absence of PhOD (Figure 4d). We conclude that the ordinary phenol is unable to quench the ^{3}MLCT excited state of $[Re(CO)_3(phen)(py)]^+$ under the experimental conditions chosen.

Figure 5 shows the results of an analogous series of experiments performed with PhOH-CH_2-py. From Figure 5a we learn that the emission intensity of $[Re(CO)_3(phen)(py)]^+$ is quenched

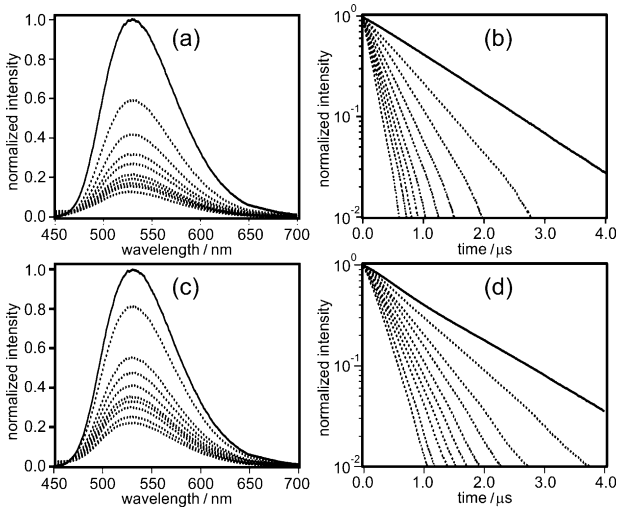

Figure 5. a) Luminescence of $[Re(CO)_3(phen)(py)]^+$ in aerated CH_2Cl_2 with 100 mM CH_3OH in the absence (——) and presence of increasing amounts of PhOH-CH_2-py (•••••; 1–10 mM) after excitation at 410 nm. b) Luminescence decays of $[Re(CO)_3(phen)(py)]^+$ in the same solvent in the absence (——) and presence of increasing amounts of PhOH-CH_2-py (•••••) after excitation at 410 nm with laser pulses of width approximately 10 ns (detection wavelength: 530 nm). c) The same experiment as in (a) but with deuterated phenol (PhOD-CH_2-py) and 100 mM CH_3OD. d) The same experiment as in (b) but with deuterated phenol (PhOD-CH_2-py) and 100 mM CH_3OD. All *y* axes are in arbitrary units; the intensity of the unquenched emission in (a) and (c) is normalized arbitrarily to 1; the intensity at $t = 0$ in (b) and (d) is normalized arbitrarily to 1.

significantly in the presence of 1–10 mM PhOH-CH_2-py (dotted traces compared to solid trace). Similarly, the luminescence decays are strongly dependent on the PhOH-CH_2-py concentration (Figure 5b). On using deuterated PhOD-CH_2-py the luminescence decays (Figure 5d) are noticeably slower than for undeuterated PhOH-CH_2-py at equal concentration (Figure 5b). Likewise, in the luminescence intensity data of Figure 5c, quenching at a given phenol concentration is noticeably weaker than for the undeuterated quencher in Figure 5a. Thus, there appears to be a significant H/D kinetic isotope effect (KIE).

Figure 6a is a Stern–Volmer plot based on the luminescence intensity data from Figures 4 and 5, and Figure 6b is a Stern–Volmer plot based on the luminescence lifetime data from Figures 4 and 5.[23] The open circles in Figure 6a,b represent data obtained with PhOH-CH_2-py, and the open squares represent data obtained with the deuterated analogue PhOD-CH_2-py. Linear regression fits yield the Stern–Volmer constants (K_{SV}) given in the third (ordinary phenols) and fourth columns (deuterated phenols) of Table 2.

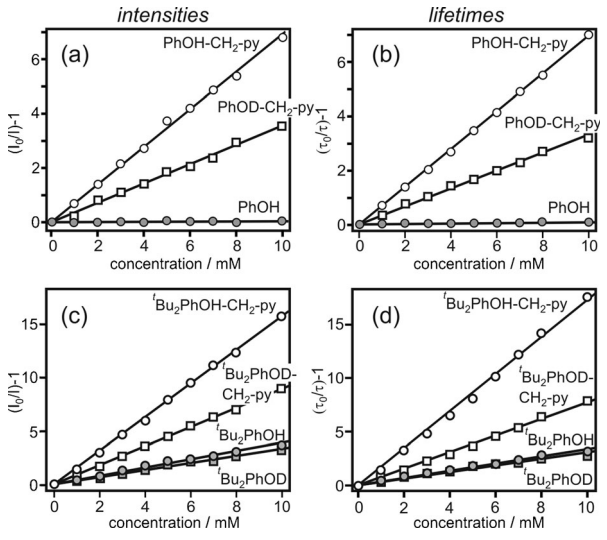

Figure 6. a) Stern–Volmer plot based on the luminescence intensity data from Figures 4 and 5; (○): PhOH-CH_2-py, (□): PhOD-CH_2-py, gray filled circles: PhOH. b) Stern–Volmer plot based on the luminescence lifetime data from Figures 4 and 5; (○): PhOH-CH_2-py, (□): PhOD-CH_2-py, gray filled circles: PhOH. c) Stern–Volmer plot based on the luminescence intensity data from Figures S1 and S2; (○): *t*Bu_2PhOH-CH_2-py, (□): *t*Bu_2PhOD-CH_2-py, gray filled circles: *t*Bu_2PhOH, gray filled squares: *t*Bu_2PhOD. d) Stern–Volmer plot based on the luminescence lifetime data from Figures S1 and S2; (○): *t*Bu_2PhOH-CH_2-py, (□): *t*Bu_2PhOD-CH_2-py, gray filled circles: *t*Bu_2PhOH, gray filled squares: *t*Bu_2PhOD.

Table 2. Results from luminescence quenching experiments.

Phenol	Exp. type	$K_{SV,H}$ [M^{-1}][a]	$K_{SV,D}$ [M^{-1}][a]	$k_{Q,H}$ [$M^{-1}s^{-1}$][b]	$k_{Q,D}$ [$M^{-1}s^{-1}$][b]	KIE[c]
PhOH/D	intensity	3.4±1.2	0.5±3.7	(2.9±1.0)×10^6	(0.4±3.1)×10^6	N/A
	lifetime	8.4±0.4	13.8±1.0	(7.1±0.3)×10^6	(11.7±0.8)×10^6	N/A
PhOH/D-CH_2-py	intensity	691±7	355±5	(5.9±0.1)×10^8	(3.0±0.1)×10^8	2.0±0.1
	lifetime	701±3	334±6	(5.9±0.1)×10^8	(2.8±0.1)×10^8	2.1±0.1
tBu_2PhOH/D	intensity	391±8	332±8	(3.3±0.1)×10^8	(2.8±0.1)×10^8	1.2±0.1
	lifetime	437±11	309±10	(3.7±0.1)×10^8	(2.6±0.1)×10^8	1.4±0.1
tBu_2PhOH/D-CH_2-py	intensity	1572±9	892±5	(13.3±0.1)×10^8	(7.6±0.1)×10^8	1.8±0.1
	lifetime	1648±8	773±8	(14.0±0.1)×10^8	(6.6±0.1)×10^8	2.1±0.1

[a] Stern–Volmer constants obtained from emission intensity or lifetime experiments with normal ($K_{SV,H}$) and deuterated phenols ($K_{SV,D}$). [b] Rate constants for bimolecular excited-state quenching with normal ($k_{Q,H}$) and deuterated phenols ($k_{Q,D}$); calculated from $K_{SV,H}$ and $K_{SV,D}$ values using the lifetime of ^{3}MLCT-excited [$Re(CO)_3$(phen)(py)]$^+$ in aerated CH_2Cl_2 with 100 mM CH_3OH (1177 ns). [c] H/D kinetic isotope effect calculated from the ratio of $k_{Q,H}$ and $k_{Q,D}$.

The H/D KIE mentioned above shows up directly in the Stern–Volmer constants. From the intensity data in Figure 6 one extracts $K_{SV,H}=691\pm7\,M^{-1}$ (for PhOH-CH_2-py) and $K_{SV,D}=355\pm5\,M^{-1}$ (for PhOD-CH_2-py); the lifetime data in Figure 6b yield $K_{SV,H}=701\pm3\,M^{-1}$ (for PhOH-CH_2-py) and $K_{SV,D}=334\pm6\,M^{-1}$ (for PhOD-CH_2-py). Based on the ^{3}MLCT lifetime of [$Re(CO)_3$(phen)(py)]$^+$ (1.2 μs in aerated CH_2Cl_2, see above), we calculate rate constants for bimolecular excited-state quenching of $k_{Q,H}=(5.9\pm0.1)\times10^8\,M^{-1}s^{-1}$ for PhOH-CH_2-py and $k_{Q,D}=(2.8\pm0.1)\times10^8\,M^{-1}s^{-1}$ for PhOD-CH_2-py (fifth and sixth columns of Table 2).[23] The H/D KIE is the ratio between $k_{Q,H}$ and $k_{Q,D}$ and amounts to 2.1±0.1 (last column of Table 2).[6g] From the luminescence intensity data in Figure 6a one extracts $k_{Q,H}=(5.9\pm0.1)\times10^8\,M^{-1}s^{-1}$ for PhOH-CH_2-py and $k_{Q,D}=(3.0\pm0.1)\times10^8\,M^{-1}s^{-1}$ for PhOD-CH_2-py, yielding a value of KIE (2.0±0.1) in accordance with the lifetime data.

The gray filled circles in Figure 6a,b represent data obtained for the undeuterated reference phenol PhOH. One extracts $K_{SV,H}=3.4\pm1.2\,M^{-1}$ from the intensity data in Figure 6a and $K_{SV,H}=8.4\pm0.4\,M^{-1}$ from the lifetime data in Figure 6b, which in turn yields $k_{Q,H}$ values on the order of $10^6\,M^{-1}s^{-1}$. This order of magnitude of $k_{Q,H}$ underscores what in principle is already evident from the raw data in Figure 4: reductive excited-state quenching by PhOH is not kinetically competitive with other (radiative and nonradiative) deactivation processes of photoexcited [$Re(CO)_3$(phen)(py)]$^+$. Thus, even though $k_{Q,D}$ values for deuterated phenol are technically available from the data in Figure 4c,d, calculation of an H/D KIE is not meaningful in the case of the simple reference phenol.

Figure 6c,d shows Stern–Volmer plots based on [$Re(CO)_3$(phen)(py)]$^+$ luminescence quenching experiments with *t*Bu_2PhOH (gray filled circles), *t*Bu_2PhOD (gray filled squares), *t*Bu_2PhOH-CH_2-py (open circles), and *t*Bu_2PhOD-CH_2-py (open squares). The respective raw data are shown in Figures S1 and S2 of the Supporting Information. The bimolecular rate constants for excited-state quenching with *t*Bu_2PhOH and its deuterated congener extracted from these data are all around $3\times10^8\,M^{-1}s^{-1}$ (Table 2); for *t*Bu_2PhOH/D-CH_2-py the k_Q values are about a factor of 3 larger. H/D KIEs range from close to 1.0 for *t*Bu_2PhOH to about 2.0 for *t*Bu_2PhOH-CH_2-py.

All luminescence quenching experiments were performed in the presence of 100 mM CH_3OH/CD_3OD to ensure deuteration of the phenol molecules for the KIE studies. Use of pure CH_2Cl_2 or CD_2Cl_2 leads to markedly lower KIEs, presumably due to D/H exchange of the deuterated phenols if brought into contact with glassware/cuvettes.

Figure 7 shows a plot of the (average) k_Q values versus standard Gibbs free energy of reac-

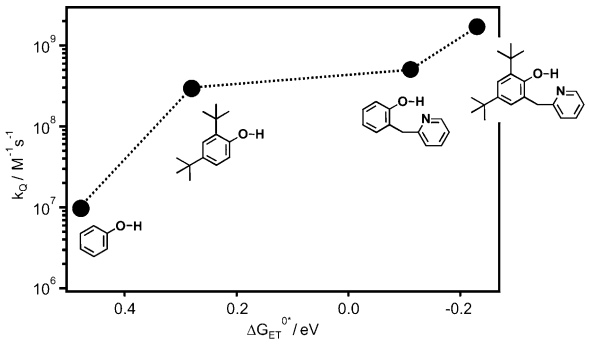

Figure 7. Rate constant ($k_{Q,H}$; from Table 2) for ^{3}MLCT excited-state quenching of [$Re(CO)_3$(phen)(py)]$^+$ versus driving force for reductive excited-state quenching (ΔG_{ET}^{0*}; estimated on the basis of the data in Table 1).

tion ($\Delta G_{ET}^{\circ *}$) associated with ET from the individual phenols to ^{3}MLCT-excited $[Re(CO)_3(phen)(py)]^+$. The free energies were calculated based on the redox potentials from Table 1, using the previously determined electrochemical potential for one-electron reduction of photoexcited $[Re(CO)_3(phen)(py)]^+$ of 0.77 V versus Fc^+/Fc (bottom row of Table 1).[6f]

Transient Absorption

Figure 8a shows the transient absorption spectrum obtained from an acetonitrile solution with 6.7×10^{-5} M $[Re(CO)_3(phen)(py)]^+$ and 10 mM tBu$_2$PhOH-CH$_2$-py. Selective excitation of the rhenium(I) complex occurred at 355 nm (Figure 2) with laser pulses of width approximately 10 ns. The

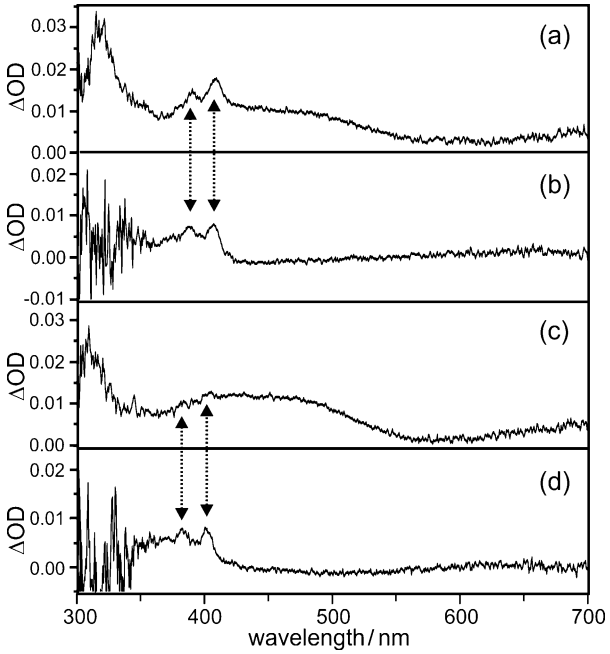

Figure 8. Transient absorption spectra measured in a time window ranging from 0 to 200 ns after excitation with 10 ns laser pulses at 355 nm. a) 6.7×10^{-5} M CH_3CN solution of $[Re(CO)_3(phen)(py)]^+$ with 10 mM tBu$_2$PhOH-CH$_2$-py; b) 2 mM CH_3CN solution of tBu$_2$PhOH-CH$_2$-py with 5 mM 1,4-dicyanonaphthalene and 0.3 M biphenyl; this set of data was detected with a time delay of 6.6 μs after the excitation pulses. c) 6.7×10^{-5} M CH_3CN solution of $[Re(CO)_3(phen)(py)]^+$ with 19.6 mM PhOH-CH$_2$-py; d) 2.1 mM CH_3CN solution of PhOH-CH$_2$-py with 5 mM 1,4-dicyanonaphthalene and 0.3 M biphenyl; this set of data was also detected with a time delay of 6.6 μs after the excitation pulses. OD = optical density.

data were time-averaged in a window ranging from 0 to 200 ns after the excitation pulse. The spectrum in Figure 8a exhibits the signatures of the reduced rhenium tricarbonyl diimine complex and neutral phenoxyl radical at the same time. The intense narrow band centered around 315 nm and the weaker featureless band extending from about 340 nm to nearly 550 nm is typical for the one-electron reduced form of the rhenium complex considered here.[6e,24] On the other hand, the narrow peaks at 390 and 409 nm (dashed vertical arrows) are due to the phenoxyl radical as becomes evident from comparison with the spectrum in Figure 8b. The latter spectrum was recorded after 355 nm excitation of a CH_3CN solution containing 2 mM tBu$_2$PhOH-CH$_2$-py, 5 mM 1,4-dicyanonaphthalene, and 0.3 M biphenyl. These reaction conditions (making use of 1,4-dicyanonaphthalene as a photosensitizer and biphenyl as a co-donor) represent an efficient means for the photogeneration of neutral phenoxyl radicals.[25] In the presence of phenol the spectral signatures of reduced 1,4-dicyanonaphthalene and oxidized biphenyl disappear within 6 μs, and hence on detecting with a delay of 6.6 μs after the 10 ns laser pulse one obtains the spectrum shown in Figure 8b, which represents the absorption spectrum of the phenoxyl radical of tBu$_2$PhOH-CH$_2$-py.[25,26] The observation of the same spectral features in Figure 8a is direct evidence for a PCET reaction, since one detects the oxidized and deprotonated form of the phenol in addition to the reduced form of the rhenium(I) reaction partner. The proton acceptor site is most likely the pyridine unit of tBu$_2$PhOH-CH$_2$-py but this cannot be monitored by transient absorption spectroscopy.

Figure 8c,d shows data from experiments that are analogous to those in Figure 8a,b but using solutions with PhOH-CH$_2$-py instead of tBu$_2$PhOH-CH$_2$-py. Qualitatively similar transient absorption spectra are obtained, but the phenoxyl radical signals are markedly weaker for PhOH-CH$_2$-py than for tBu$_2$PhOH-CH$_2$-py. However, careful inspection of the data in Figure 8c reveals that the respective signals, observed at 382 and 402 nm in Figure 8d, are indeed detectable in the rhenium/PhOH-CH$_2$-py mixture (dashed vertical arrows). Note that phenoxyl radicals typically have extinction coefficients on the order of 3000 L mol^{-1} cm^{-1},[26] hence the weakness of some of the signals in Figure 8 is not particularly unusual. The data provide direct evidence for PCET photoproducts in both rhenium(I)/pyridylphenol reaction couples.

3. Conclusions

The hydrogen-bonded pyridylphenols from Scheme 1 quench the ^{3}MLCT excited state of $[Re(CO)_3(phen)(py)]^+$ at significantly higher rates than ordinary reference phenols. This observation is in line with the substantially lower oxidation potentials (approximately 0.5 V) of the pyridylphenols relative to the reference phenols. The lower oxidation potentials in turn are the result of proton-coupled oxidation processes, as demonstrated in prior studies.[2e,5d,n] Thus, we conclude that in the PhOH-CH$_2$-py/rhenium(I) and tBu$_2$PhOH-CH$_2$-py/rhenium(I) reaction couples considered herein the overall quenching process is a CPET reaction involving ET from the phenols to the photoexcited metal complex and transfer of the phenolic proton to the pyridine base. Transient absorption data support this conclusion because they provide direct evidence for the photogeneration of neutral phenoxyl radicals. H/D KIEs on the order of 2 point to the involvement of CPET in the excited-state chemistry, in line with the prior notion that the oxidation potentials of the pyridylphenols can only be that much lower than those of ordinary phenols (approximately 0.5 V) because electron release is inherently coupled to deprotonation.[2e,5d,n]

Interestingly, excited-state quenching with tBu$_2$PhOH by simple ET is already quite efficient ($(3.3\pm0.1)\times10^8$ M^{-1} s^{-1}), yet

tBu_2PhOH-CH_2-py quenches the rhenium ^{3}MLCT state even more rapidly ($(13.3\pm0.1)\times10^8\ M^{-1}s^{-1}$) and with an H/D KIE of approximately 2, which suggests that CPET stays kinetically highly competitive with an ET/PT sequence even in a situation in which the initial ET step is thermodynamically possible.

Experimental Section

A suspension of NaH (60% in mineral oil, 1.20 g, 30 mmol) in anhydrous THF (6 mL) was cooled to 0 °C and a solution of 2-bromophenol (**1**; 3.44 g, 20 mmol) in anhydrous THF (8 mL) was added dropwise over 1 h under N_2 atmosphere. After stirring for an additional 10 min, iodomethane (9.2 g, 64.8 mmol) was added and the mixture was allowed to warm up to room temperature prior to heating at reflux for 19 h. After cooling to room temperature, water (160 mL) was added and the product was extracted with pentane (3×100 mL). The combined organic phases were dried over anhydrous $MgSO_4$, and the solvent was removed on a rotary evaporator. Subsequent purification on silica gel with CH_2Cl_2 as eluent ($R_f\approx0.3$) gave 1-bromo-2-methoxybenzene (**2**) in 97% yield.[27] ^{1}H NMR (300 MHz, $CDCl_3$): $\delta=3.89$ (s, 3H), 6.78–6.95 (m, 2H), 7.27 (td, $J=8.2$, 6.1 Hz, 1H), 7.54 ppm (dd, $J=7.8$, 1.6 Hz, 1H).

The same procedure using identical molar quantities of starting materials was employed for the synthesis of 1-bromo-3,5-di-*tert*-butyl-2-methoxybenzene (**4**) from 2-bromo-4,6-di-*tert*-butylphenol (**3**). On silica gel with CH_2Cl_2 as eluent, product **4** had $R_f\approx0.6$ and the yield was 97%. ^{1}H NMR (300 MHz, $CDCl_3$): $\delta=1.30$ (s, 9H), 1.40 (s, 9H), 3.91 (s, 3H), 7.28 (d, $J=2.4$ Hz, 1H), 7.41 ppm (d, $J=2.4$ Hz, 1H).

For the synthesis of molecule **5** a solution of 2-picoline (200 mmol) in anhydrous THF (200 mL) was cooled to −30 °C and 1.6 M *n*-butyllithium in hexane (200 mmol) was added slowly. After stirring at this temperature for 30 min, diisopropyl ketone was added slowly and the reaction mixture was stirred for another 2 h at room temperature. Subsequently water (300 mL) was added and the resulting mixture was extracted with ethyl acetate (3×200 mL). The combined organic phases were dried over anhydrous $MgSO_4$, and the solvent was removed with a rotary evaporator. The raw product was purified by column chromatography on silica gel using a 3:1 (v/v) mixture of pentane and ethyl acetate as eluent ($R_f\approx0.6$). This procedure afforded pure **5** in 83% yield.[8] ^{1}H NMR (300 MHz, $CDCl_3$): $\delta=0.88$ (dd, $J=6.9$, 4.9 Hz, 12H), 1.90 (m, 2H), 2.98 (s, 2H), 6.29 (s, 1H), 7.08–7.13 (m, 1H), 7.15 (d, $J=7.8$ Hz, 1H), 7.58 (td, $J=7.7$, 1.9 Hz, 1H), 8.43 ppm (ddd, $J=4.9$, 1.8, 0.9 Hz, 1H).

Using a heat gun Cs_2CO_3 (27.90 g, 85.6 mmol) was dried under vacuum. Subsequently, palladium trifluoroacetate (1.18 g, 3.6 mmol), tricyclohexylphosphine (2.00 g, 7.1 mmol), dry *p*-xylene (150 mL), 1-bromo-2-methoxybenzene (**2**; 16.00 g, 85.6 mmol), and pyridine **5** (14.70 g, 71.3 mmol) were added under nitrogen. The reaction mixture was heated at reflux under N_2 overnight. After cooling to room temperature the mixture was filtered, and the solvent was evaporated under reduced pressure. Column chromatography on silica gel using a 5:1 (v/v) mixture of pentane and ethyl acetate ($R_f\approx0.1$) afforded the coupling product **6** as a yellow liquid in 73% yield.[8] ^{1}H NMR (300 MHz, $CDCl_3$): $\delta=3.80$ (s, 3H), 4.17 (s, 2H), 6.90 (ddd, $J=8.1$, 6.3, 2.6 Hz, 2H), 7.03–7.14 (m, 2H), 7.14–7.26 (m, 2H), 7.54 (td, $J=7.7$, 1.9 Hz, 1H), 8.49–8.58 ppm (m, 1H).

Molecule **6** (0.15 g, 0.78 mmol) was dissolved in aqueous HBr (47%, 4 mL) and the mixture was heated at reflux for 19 h.[9] After evaporation of excess acid, water was added to the solid residue, and the solution was neutralized by addition of an aqueous K_2CO_3 solution. The product (**7**) was extracted with CH_2Cl_2, and the combined organic phases were dried over anhydrous $MgSO_4$ prior to solvent removal on a rotary evaporator. The raw product was purified by column chromatography on silica gel with CH_2Cl_2 as eluent ($R_f\approx0.4$) affording product **7** (PhOH-CH_2-py) as a white solid in 57% yield. ^{1}H NMR (300 MHz, $CDCl_3$): $\delta=4.10$ (s, 2H), 6.82 (td, $J=7.4$, 1.3 Hz, 1H), 6.95–7.02 (m, 1H), 7.13–7.21 (m, 3H), 7.32 (d, $J=7.8$ Hz, 1H), 7.69 (td, $J=7.7$, 1.8 Hz, 1H), 8.46 (ddd, $J=5.0$, 1.8, 0.8 Hz, 1H), 11.67 ppm (s, 1H); ^{13}C NMR (75 MHz, $CDCl_3$): $\delta=41.7$, 118.5, 119.9, 121.9, 122.8, 126.2, 128.7, 130.2, 138.2, 147.8, 156.7, 161.0 ppm; MS (EI): *m/z* (%): found: 186.0921 $[M+H]^+$, calcd: 186.0913; elemental analysis calcd (%) for $C_{13}H_{13}NO$: C 77.81, H 5.99, N 7.56; found: C 77.63, H 5.97, N 7.47.

For the synthesis of molecule **8** from 1-bromo-3,5-di-*tert*-butyl-2-methoxybenzene (**4**) and pyridine **5**, the same procedure as that described above for molecule **6** was employed.[8] The quantities of reactants used in this case were as follows: Cs_2CO_3: 22.81 g, 70.0 mmol; palladium trifluoroacetate: 0.97 g, 2.9 mmol; tricyclohexylphosphine: 1.63 g, 5.8 mmol; dry *p*-xylene: 150 mL; 1-bromo-3,5-di-*tert*-butyl-2-methoxybenzene (**4**): 20.86 g, 70 mmol; pyridine **5**: 12.10 g, 58.3 mmol. Under the same chromatography conditions as described above for molecule **6**, the R_f value was approximately 0.3, and molecule **8** was obtained in 69% yield as a yellow oil. ^{1}H NMR (300 MHz, $CDCl_3$): $\delta=1.26$ (s, 9H), 1.43 (s, 9H), 3.75 (s, 3H), 4.27 (s, 2H), 6.98–7.17 (m, 3H), 7.26–7.31 (m, 1H), 7.56 (td, $J=7.7$, 1.9 Hz, 1H), 8.57 ppm (ddd, $J=4.9$, 1.8, 0.9 Hz, 1H).

On subjecting molecule **8** to the same methoxyl-deprotection reaction with aqueous HBr as described above for molecule **6**, not only the methoxyl group but also the *tert*-butyl substituents of molecule **8** were cleaved off and the reaction afforded molecule **7**. It was therefore necessary to apply the following procedure to obtain molecule **9**.[10] Ethanethiol (0.69 g, 11.2 mmol) was added dropwise to a suspension of NaH (60% in mineral oil, 0.31 g, 12.8 mmol) in dry *N*,*N*-dimethylformamide under N_2 atmosphere. Then molecule **8** (0.50 g, 1.6 mmol) was added and the reaction mixture was stirred at 100 °C overnight. After cooling to room temperature, H_2O (4 mL), 1 M aqueous HCl (13 mL), and phosphate buffer (0.5 M, pH 7) were added, and the mixture was extracted with diethyl ether (3×50 mL). The combined organic phases were dried over anhydrous $MgSO_4$, and the solvent was removed on a rotary evaporator. Purification by three successive chromatography columns on silica gel using a 7:3 (v/v) pentane/dichloromethane mixture ($R_f\approx0.5$) gave product **9** (*t*Bu_2PhOH-CH_2-py) in 65% yield as a white solid. ^{1}H NMR (300 MHz, $CDCl_3$): $\delta=1.31$ (s, 9H), 1.47 (s, 9H), 4.10 (s, 2H), 7.06 (d, $J=2.5$ Hz, 1H), 7.17 (ddd, $J=7.6$, 5.0, 1.1 Hz, 1H), 7.24 (d, $J=2.4$ Hz, 1H), 7.34 (d, $J=7.8$ Hz, 1H), 7.67 (td, $J=7.7$, 1.8 Hz, 1H), 8.45 (ddd, $J=5.0$, 1.7, 0.9 Hz, 1H), 11.40 ppm (s, 1H); ^{13}C NMR (75 MHz, $CDCl_3$): $\delta=28.8$, 30.7, 33.2, 34.1, 41.2, 120.7, 121.7, 122.0, 123.9, 125.3, 136.9, 137.0, 140.4, 146.6, 151.8, 160.5 ppm; MS (EI): *m/z* (%): found: 298.2168 $[M+H]^+$, calcd: 298.2165; elemental analysis calcd (%) for $C_{20}H_{27}NO\cdot0.1C_3H_7NO\cdot0.5C_5H_{12}$: C 80.35, H 9.97, N 4.52; found: C 80.29, H 10.02, N 4.63.

Deuteration of the phenolic functions occurred by dissolving the individual phenol molecules in a 1:1 mixture of CH_3CN and D_2O (99.9%) followed by solvent removal on a rotary evaporator; this procedure was accomplished twice to ensure high isotope purity. Luminescence quenching experiments in CH_2Cl_2 occurred in the presence of 100 mM CD_3OD (99.99%) to avoid significant D/H exchange through contact of the phenols with glassware and cuv-

ettes. For experiments with undeuterated phenols, 100 mM CH_3OH was added.

The $[Re(CO)_3(phen)(py)]^+$ complex was available from prior studies in the form of its hexafluorophosphate salt.[6e,f]

^1H and ^{13}C NMR spectra were measured on a Bruker B-ACS-120 instrument. Electron-impact mass spectrometry was carried out with a Finnigan MAT 95 spectrometer. Elemental analyses were performed with a Vario EL3 instrument. For cyclic voltammetry a Versastat3-200 potentiostat from Princeton Applied Research was used. A glassy carbon working electrode, a platinum counter electrode, and a silver quasi-reference electrode were employed. Tetrabutylammonium hexafluorophosphate ($TBAPF_6$, 0.1 M) was used as an electrolyte; prior to voltage sweeps at rates of 0.1 $V s^{-1}$ the solvent was flushed with nitrogen. Optical absorption spectra were recorded on a Cary 5000 instrument from Varian, and steady-state luminescence experiments were performed on a Fluorolog-3 apparatus from Horiba Jobin–Yvon. Luminescence lifetime experiments were performed in Geneva by using a home-built setup comprising a Quantel Brilliant Nd:YAG laser with an integrated magic prism optical parametric oscillator as an excitation source and a detection system consisting of a Spex 270M monochromator, an R928 photomultiplier from Hamamatsu, and a Tektronix TDS 540B digital oscilloscope. Transient absorption experiments were performed in Göttingen by using an LP920-KS instrument from Edinburgh Instruments equipped with an iCCD camera from Andor and a Quantel Brilliant b laser as an excitation source.

For the X-ray structures, crystals of **7** and **9** were grown by slow evaporation of the solvent at room temperature. They were selected and mounted with inert oil on a kapton MicroMount. The data for **7** were collected at 100 K on a Bruker Apex II Ultra instrument with mirror optics. The data for **9** were collected on a Bruker smart Apex II Quazar system with an Incoatec IμS source.[28] Data reduction was performed with SAINT,[29] and an empirical absorption correction with SADABS[30] was applied. The structures were solved by direct methods (SHELXS-97)[31] and refined by full-matrix least-squares methods against F^2 with SHELXL-97[31] and the ShelXle[32] graphic user interface. All non-hydrogen atoms were refined with anisotropic displacement parameters. The hydrogen atoms were refined isotropically on calculated positions by using a riding model with their U_{iso} values constrained to 1.5 times the U_{eq} of their pivot atoms for terminal sp^3 carbon atoms and 1.2 times for all other carbon atoms. Crystallographic data (excluding structure factors) for the structures reported herein have been deposited with the Cambridge Crystallographic Data Centre. The CCDC numbers, crystal data, and experimental details for the X-ray measurements are listed in the Supporting Information. CCDC 887369 (**7**) and 887370 (**9**) contain the supplementary crystallographic data for this paper. These data can be obtained free of charge from The Cambridge Crystallographic Data Centre via www.ccdc.cam.ac.uk/data_request/cif.

Acknowledgements

This research was supported by the Swiss National Science Foundation (SNSF) through grant number PP002-110611, by the Danish National Research Foundation (DNRF) funded Center for Materials Crystallography (CMC), and by the Deutsche Forschungsgemeinschaft (DFG) through IRTG-1422 and grant number INST186/872-1. The MWK Niedersachsen is thanked for co-funding the transient absorption spectrometer. J. M. Mayer and T. F. Markle are acknowledged for valuable discussions.

Keywords: electron transfer · luminescence · photochemistry · proton transfer · transient absorption

[1] a) I. Bertini, H. B. Gray, E. I. Stiefel, J. S. Valentine, *Biological Inorganic Chemistry*, University Science Books, Sausalito, **2007**; b) G. Renger, T. Renger, *Photosynth. Res.* **2008**, *98*, 53–80.

[2] a) B. A. Barry, G. T. Babcock, *Proc. Natl. Acad. Sci. USA* **1987**, *84*, 7099–7103; b) S. Y. Reece, D. G. Nocera, *Annu. Rev. Biochem.* **2009**, *78*, 673–699; c) T. J. Meyer, M. H. V. Huynh, H. H. Thorp, *Angew. Chem.* **2007**, *119*, 5378–5399; *Angew. Chem. Int. Ed.* **2007**, *46*, 5284–5304; d) M. H. V. Huynh, T. J. Meyer, *Chem. Rev.* **2007**, *107*, 5004–5064; e) J. M. Mayer, I. J. Rhile, F. B. Larsen, E. A. Mader, T. F. Markle, A. G. DiPasquale, *Photosynth. Res.* **2006**, *87*, 3–20; f) J. L. Dempsey, J. R. Winkler, H. B. Gray, *Chem. Rev.* **2010**, *110*, 7024–7039; g) S. Hammes-Schiffer, A. A. Stuchebrukhov, *Chem. Rev.* **2010**, *110*, 6939–6960; h) J. J. Warren, J. R. Winkler, H. B. Gray, *FEBS Lett.* **2012**, *586*, 596–602.

[3] a) L. Benisvy, R. Bittl, E. Bothe, C. D. Garner, J. McMaster, S. Ross, C. Teutloff, F. Neese, *Angew. Chem.* **2005**, *117*, 5448–5451; *Angew. Chem. Int. Ed.* **2005**, *44*, 5314–5317; b) T. Maki, Y. Araki, Y. Ishida, O. Onomura, Y. Matsumura, *J. Am. Chem. Soc.* **2001**, *123*, 3371–3372; c) T. Lachaud, A. Quaranta, Y. Pellegrin, P. Dorlet, M. F. Charlot, S. Un, W. Leibl, A. Aukauloo, *Angew. Chem.* **2005**, *117*, 1560–1564; *Angew. Chem. Int. Ed.* **2005**, *44*, 1536–1540.

[4] a) C. Costentin, M. Robert, J.-M. Savéant, *Acc. Chem. Res.* **2010**, *43*, 1019–1029; b) C. Costentin, M. Robert, J. M. Savéant, *J. Am. Chem. Soc.* **2006**, *128*, 4552–4553; c) J. Bonin, C. Costentin, M. Robert, J. M. Savéant, *Org. Biomol. Chem.* **2011**, *9*, 4064–4069; d) C. Costentin, M. Robert, J. M. Savéant, C. Tard, *Phys. Chem. Chem. Phys.* **2011**, *13*, 5353–5358; e) J. Bonin, C. Costentin, C. Louault, M. Robert, M. Routier, J. M. Savéant, *Proc. Natl. Acad. Sci. USA* **2010**, *107*, 3367–3372; f) C. Costentin, M. Robert, J. M. Savéant, C. Tard, *Angew. Chem.* **2010**, *122*, 3891–3894; *Angew. Chem. Int. Ed.* **2010**, *49*, 3803–3806.

[5] a) G. F. Moore, M. Hambourger, M. Gervaldo, O. G. Poluektov, T. Rajh, D. Gust, T. A. Moore, A. L. Moore, *J. Am. Chem. Soc.* **2008**, *130*, 10466–10467; b) S. Y. Reece, D. G. Nocera, *J. Am. Chem. Soc.* **2005**, *127*, 9448–9458; c) I. J. Rhile, T. F. Markle, H. Nagao, A. G. DiPasquale, O. P. Lam, M. A. Lockwood, K. Rotter, J. M. Mayer, *J. Am. Chem. Soc.* **2006**, *128*, 6075–6088; d) I. J. Rhile, J. M. Mayer, *J. Am. Chem. Soc.* **2004**, *126*, 12718–12719; e) T. F. Markle, I. J. Rhile, A. G. DiPasquale, J. M. Mayer, *Proc. Natl. Acad. Sci. USA* **2008**, *105*, 8185–8190; f) T. F. Markle, J. M. Mayer, *Angew. Chem.* **2008**, *120*, 750–752; *Angew. Chem. Int. Ed.* **2008**, *47*, 738–740; g) A. Magnuson, M. Anderlund, O. Johansson, P. Lindblad, R. Lomoth, T. Polivka, S. Ott, K. Stensjö, S. Styring, V. Sundström, L. Hammarström, *Acc. Chem. Res.* **2009**, *42*, 1899–1909; h) O. Johansson, H. Wolpher, M. Borgström, L. Hammarström, J. Bergquist, L. C. Sun, B. Åkermark, *Chem. Commun.* **2004**, 194–195; i) L. Hammarström, S. Styring, *Energy Environ. Sci.* **2011**, *4*, 2379–2388; j) A. Magnuson, H. Berglund, P. Korall, L. Hammarström, B. Åkermark, S. Styring, L. C. Sun, *J. Am. Chem. Soc.* **1997**, *119*, 10720–10725; k) M. Sjödin, T. Irebo, J. E. Utas, J. Lind, G. Merenyi, B. Åkermark, L. Hammarström, *J. Am. Chem. Soc.* **2006**, *128*, 13076–13083; l) L. C. Sun, M. Burkitt, M. Tamm, M. K. Raymond, M. Abrahamsson, D. LeGourriérec, Y. Frapart, A. Magnuson, P. H. Kenéz, P. Brandt, A. Tran, L. Hammarström, S. Styring, B. Åkermark, *J. Am. Chem. Soc.* **1999**, *121*, 6834–6842; m) M.-T. Zhang, T. Irebo, O. Johansson, L. Hammarström, *J. Am. Chem. Soc.* **2011**, *133*, 13224–13227; n) T. F. Markle, I. J. Rhile, J. M. Mayer, *J. Am. Chem. Soc.* **2011**, *133*, 17341–17352.

[6] a) C. J. Gagliardi, B. C. Westlake, C. A. Kent, J. J. Paul, J. M. Papanikolas, T. J. Meyer, *Coord. Chem. Rev.* **2010**, *254*, 2459–2471; b) O. S. Wenger, *Chem. Eur. J.* **2011**, *17*, 11692–11702; c) T. Irebo, S. Y. Reece, M. Sjödin, D. G. Nocera, L. Hammarström, *J. Am. Chem. Soc.* **2007**, *129*, 15462–15464; d) B. C. Westlake, M. K. Brennaman, J. J. Concepcion, J. J. Paul, S. E. Bettis, S. D. Hampton, S. A. Miller, N. V. Lebedeva, M. D. E. Forbes, A. M. Moran, T. J. Meyer, J. M. Papanikolas, *Proc. Natl. Acad. Sci. USA* **2011**, *108*, 8554–8558; e) M. Kuss-Petermann, H. Wolf, D. Stalke, O. S. Wenger, *J. Am. Chem. Soc.* **2012**, *134*, 12844–12854; f) C. Bronner, O. S.

Wenger, *Inorg. Chem.* **2012**, *51*, 8275 – 8283; g) C. Bronner, O. S. Wenger, *J. Phys. Chem. Lett.* **2012**, *3*, 70 – 74; h) O. S. Wenger, *Acc. Chem. Res.* **2013**, DOI:10.1021/ar300289x.
[7] W. B. Connick, A. J. Di Bilio, M. G. Hill, J. R. Winkler, H. B. Gray, *Inorg. Chim. Acta* **1995**, *240*, 169 – 173.
[8] T. Niwa, H. Yorimitsu, K. Oshima, *Angew. Chem.* **2007**, *119*, 2697 – 2699; *Angew. Chem. Int. Ed.* **2007**, *46*, 2643 – 2645.
[9] O. Mongin, P. Rocca, L. Thomas-dit-Dumont, F. Trécourt, F. Marsais, A. Godard, G. Quéguiner, *J. Chem. Soc. Perkin Trans. 1* **1995**, 2503 – 2508.
[10] V. Diemer, H. Chaumeil, A. Defoin, A. Fort, A. Boeglin, C. Carré, *Eur. J. Org. Chem.* **2008**, 1767 – 1776.
[11] a) T. Steiner, *Angew. Chem.* **2002**, *114*, 50 – 80; *Angew. Chem. Int. Ed.* **2002**, *41*, 48 – 76; b) J. Overgaard, B. B. Iversen, *Struct. Bonding* **2012**, *146*, 53 – 74; c) G. R. Desiraju, T. Steiner, *The Weak Hydrogen Bond*, Oxford University Press, Oxford, **1999**.
[12] R. M. Silverstein, C. Bassler, T. C. Morrill, *Spectrometric Identification of Organic Compounds, 5th ed.*, Wiley, New York, **1991**.
[13] F. G. Bordwell, J. P. Cheng, *J. Am. Chem. Soc.* **1991**, *113*, 1736 – 1743.
[14] T. F. Markle, A. L. Tenderholt, J. M. Mayer, *J. Phys. Chem. B* **2012**, *116*, 571 – 584.
[15] M. Yamaji, J. Oshima, M. Hidaka, *Chem. Phys. Lett.* **2009**, *475*, 235 – 239.
[16] V. V. Pavlishchuk, A. W. Addison, *Inorg. Chim. Acta* **2000**, *298*, 97 – 102.
[17] I. Vedernikova, J. P. Tollenaere, A. Haemers, *J. Phys. Org. Chem.* **1999**, *12*, 144 – 150.
[18] V. W. Manner, T. F. Markle, J. H. Freudenthal, J. P. Roth, J. M. Mayer, *Chem. Commun.* **2008**, 256 – 258.
[19] a) L. Sacksteder, A. P. Zipp, E. A. Brown, J. Streich, J. N. Demas, B. A. DeGraff, *Inorg. Chem.* **1990**, *29*, 4335 – 4340; b) L. Wallace, D. P. Rillema, *Inorg. Chem.* **1993**, *32*, 3836 – 3843; c) K. S. Schanze, D. B. MacQueen, T. A. Perkins, L. A. Cabana, *Coord. Chem. Rev.* **1993**, *122*, 63 – 89.
[20] J. A. Joule, K. Mills, *Heterocyclic Chemistry, 3rd ed.*, Blackwell Science, Oxford, **2004**.
[21] P. K. Das, M. V. Encinas, J. C. Scaiano, *J. Am. Chem. Soc.* **1981**, *103*, 4154 – 4162.
[22] M. E. Walther, O. S. Wenger, *Dalton Trans.* **2008**, 6311 – 6318.
[23] D. M. Roundhill, *Photochemistry and Photophysics of Metal Complexes*, Plenum, New York, **1994**.
[24] S. Zális, C. Consani, A. E. Nahhas, A. Cannizzo, M. Chergui, F. Hartl, A. Vlcek, *Inorg. Chim. Acta* **2011**, *374*, 578 – 585.
[25] T. A. Gadosy, D. Shukla, L. J. Johnston, *J. Phys. Chem. A* **1999**, *103*, 8834 – 8839.
[26] P. K. Das, M. V. Encinas, S. Steenken, J. C. Scaiano, *J. Am. Chem. Soc.* **1981**, *103*, 4162 – 4166.
[27] J. T. Kendall, *J. Labelled Compd. Radiopharm.* **2000**, *43*, 917 – 924.
[28] T. Schulz, K. Meindl, D. Leusser, D. Stern, J. Graf, C. Michaelsen, M. Ruf, G. M. Sheldrick, D. Stalke, *J. Appl. Crystallogr.* **2009**, *42*, 885 – 891.
[29] SAINT v7.68A, Bruker, WI, USA: Madison, **2009**.
[30] G. M. Sheldrick, SADABS 2008/2, Göttingen, **2008**.
[31] G. M. Sheldrick, *Acta Cryst. A* **2008**, *64*, 112 – 122.
[32] C. B. Hübschle, G. M. Sheldrick, B. Dittrich, *J. Appl. Crystallogr.* **2011**, *44*, 1281 – 1284.

Received: December 20, 2012
Published online on February 22, 2013